



Simulation study of structural variation of metallic nanoparticles caused by hydrogenation

Hiroshi Ogawa

National Institute of Advanced Industrial Science and Technology (NRI-AIST), Umezono, Tsukuba 305-8568 Japan

ARTICLE INFO

Article history:

Received 23 July 2010

Received in revised form 1 December 2010

Accepted 3 December 2010

Available online 13 December 2010

Keywords:

Hydrogen storage

Nanoparticle

Molecular dynamics

Lattice deformation

P–C isotherms

ABSTRACT

Hydrogen absorption in b.c.c. and f.c.c. nanoparticles was investigated using molecular dynamics simulation with systematic variance of the M–H potential function parameters. Three patterns of hydrogen distribution in nanoparticles, non-absorbing, homogeneous absorbing, and forming a hydrogen-rich surface layer were observed depending on the assumed potential parameter values. Simulated P–C isotherms of nanoparticles show similarity with experimental ones. Variation of the metallic lattice because of hydrogenation was observed as transitions to b.c.t., icosahedral, or amorphous phases. Generation of grain boundary was observed to accompany these lattice transformations. The simulated P–C isotherms and structural variation were discussed in relation to the assumed potential parameters, temperature, and particle size.

© 2010 Elsevier B.V. All rights reserved.

1. Introduction

Metallic nanoparticles have been regarded as potentially useful materials for hydrogen storage because of the large surface area relative to the bulk region, which is advantageous for hydrogen absorption and desorption. Hydrogen absorption in nanoparticles has been studied mainly on Pd nanoparticles [1–9]. Pundt and coworkers [6,7] reported that the crystal structure in Pd nanoparticles varies by hydrogenation depending on the cluster size. Yamauchi et al. [8,9] showed that the P–C isotherms of Pd nanoparticles differ from those in the bulk and showed that they vary depending also on particle size. The author recently conducted classical MD studies of hydrogen absorption in 10 nm, metallic nanoparticles to elucidate the fundamental variations of hydrogen distribution and structure variation in nanoparticles as ‘parameter physics’. In this paper, the author describes extension of the particle size range to 1–10 nm to discuss the particle size dependencies of structural variation by hydrogenation and the resulting P–C isotherms.

2. MD simulation

A computational model composed of isolated nanoparticles located at the center of cubic, periodic MD cells and surrounding hydrogen gas was considered [10]. The simulated particles were 10, 8, 6, 4, 2, 1.4, and 1 nm diameter; the corresponding numbers of

metallic atoms vary from about 44 000 to 59 in b.c.c. or 55 in f.c.c. cases. The particle shape was assumed to be spherical, but it was polyhedral for smaller particles. The number of hydrogen atoms is about 40 000. They were arranged initially in the face-centered cubic lattice with lattice constants of 0.3 nm within an octahedral space at the corner of the periodic cell [10]. After starting MD calculation, hydrogen atoms evaporate rapidly from the octahedral crystal because of the H–H repulsive forces. They form a homogeneous gas phase outside the nanoparticles. The side length of the cubic MD cell was assumed to be 12, 13, 16, 20, or 25 nm to simulate various hydrogen pressures.

The potential energy of the system, E , is expressed as

$$E = \frac{1}{2} \sum_{ij} V^{i-j}(r_{ij}) + \sum_i F(\rho_i), \quad (1)$$

where V^{i-j} stands for the pair potential between atoms i and j as a function of the distance r_{ij} , F signifies the embedded function, and ρ_i denotes the electronic density at atom i because of the surrounding atoms. Each term in Eq. (1) can be considered as the variable part for the parameter physics [10], which is useful for investigating the hydrogen storage mechanisms. In our studies, only the metal–H pair term, V^{M-H} , is assumed to be variable. The metal–metal interactions were fixed to be those for b.c.c. iron and f.c.c. nickel proposed respectively by Finnis and Sinclair [13] and Ackland et al. [14]. The metal–H pair interaction is assumed to be variable in the form of

$$V^{M-H}(r + \Delta r) = \varepsilon V^{Ruda}(r), \quad (2)$$

E-mail address: ogawa@aist.go.jp

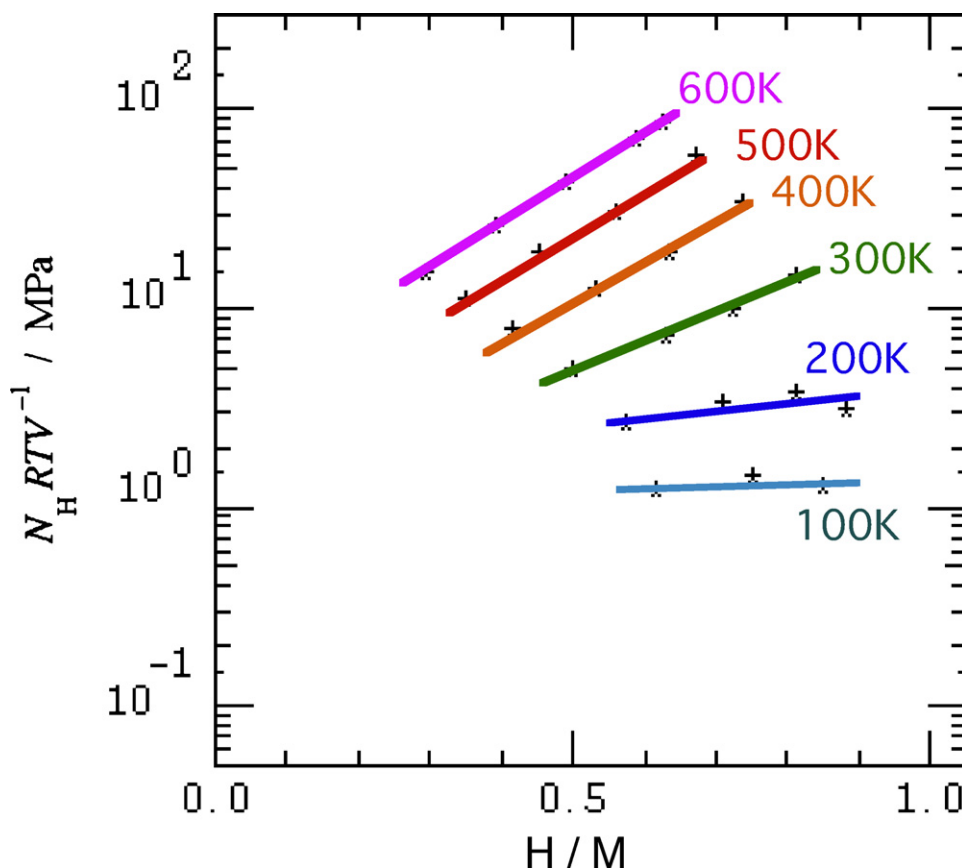


Fig. 1. Temperature dependence of simulated P–C isotherms of 10 nm, b.c.c. nanoparticles. Assumed conditions are $\varepsilon = 4$ and $\Delta r = -1$ Å.

where ε and Δr are parameters. Meanings of ε and Δr are the strength factor and bond length difference of assumed M–H bonds compared with those in the reference system. Actually, ε larger than unity produces strong M–H bonds. Negative Δr gives small H atoms with high mobility in interstitial spaces. The variation of ε and Δr causes a different balance between M–M and M–H interactions, which are expected to affect the structure of hydrogenated particles. As the reference function for V^{M-H} , we used the potential function V^{Ruda} proposed by Ruda et al. [15] for Fe–H and Ni–H pairs expressed as

$$V^{\text{Ruda}}(r) = \sum_k a_k (r_{ak} - r)^3 H(r_{ak} - r), \quad (3)$$

where H is the Heaviside step function and a_k and r_{ak} are the coefficients of polynomial fittings. For parameter physics, we assume the values $\Delta r = -0.5, -1$ and -1.5 Å and $\varepsilon = 1, 2, 4, 6, 8$, and 10 . Preliminary analyses show that the absorption energy of H atoms in the parameter range varies respectively from 4 to -80 kJ/mol H and from -21 to -309 kJ/mol H for b.c.c. and f.c.c. crystals. They cover the experimental values of real metallic elements such as Cr, V, Nb, Pd, and Sr [16]. It is noteworthy that the atomic weight of Fe or Ni was assumed; consequently, the time scale of lattice vibration is constrained by the value. The H–H pair interaction is also fixed to one with monotonic repulsion [15]. The EAM part related to H atoms was omitted to avoid awkward adjustment between the parameter-dependent pair part and the EAM part. Using this treatment, we can analyze the parameter-dependent variation more clearly. The use of repulsion-type potential results hydrogen in the gas phase in present calculation to be in the monoatomic phase. Therefore, we should limit our discussion of hydrogen dynamics after adsorption at the surface only. The MD simulation was con-

ducted using a constant-NVT condition with velocity scaling for 100 ps, which is sufficient for equilibration of H atom in 10 nm particles [11,12]. The system temperature was assumed as 100–600 K.

3. Results and discussion

3.1. General features of hydrogenation in metallic nanoparticles

As described in a previous report [10], hydrogen absorption in nanoparticles was found to be classified into three patterns: non-absorbing, homogeneous absorbing, and heterogeneous absorbing (forming surface layer). The non-absorbing case appears in the combination of potential parameters with larger ε (6, 8, and 10) and larger Δr (-0.5 Å). The heterogeneous absorbing case appears in a region with larger ε (8 and 10) and middle Δr (-1 Å). The homogeneous absorbing case appears in the remaining part of the parameter combination. Actually, MD simulation provides atomistic information not only for hydrogen distribution but also variation of the metallic lattice. Formation of the hydrogen-rich surface layer is sometimes accompanied by generation of grain boundaries inside the nanoparticles [11,12]. When the M–H interaction is weak (ε is small), twin boundaries are generated inside nanoparticles through hydrogenation. Such twin boundaries are considered to result from the cooperative motions of lattice deformation. The twin boundaries migrated in opposite directions to reduce their interface area. Some disappeared after a sufficient time. When the M–H interaction is strong (ε is large), complex 3-D configurations of grain boundaries appeared in nanoparticles and remained persistently during the simulation. Such complex grain boundaries are generated as a result of heterogeneous lattice deformation because of the hydrogen-rich surface layer.

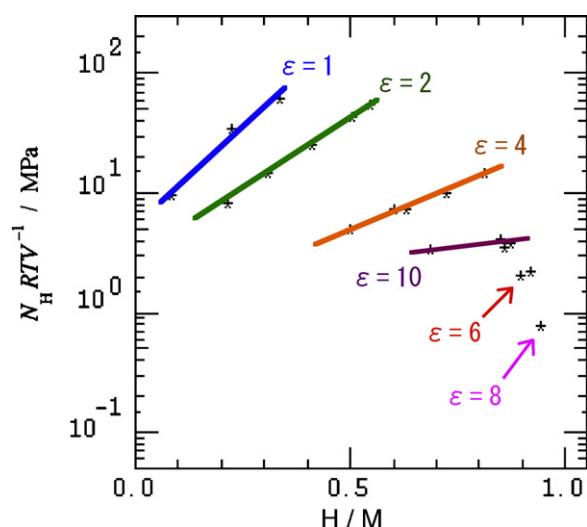


Fig. 2. Energy parameter ε dependence of simulated P–C isotherms of 10 nm, b.c.c. nanoparticles. Assumed conditions are $\Delta r = -1 \text{ \AA}$ and 300 K.

3.2. Simulated P–C isotherms of hydrogenation in nanoparticles

The P–C isotherm is a fundamental property of hydrogen storage materials. It represents the relation between hydrogen pressure and amount of absorbing hydrogen in materials (H/M ratio) at each temperature. In the atomistic simulation, we can evaluate the pressure of hydrogen gas and H/M ratio in nanoparticles respectively by counting the quantities of hydrogen atoms outside and inside the nanoparticles. Therefore, P–C isotherms can be evaluated by systematic change in the number of hydrogen atoms in the MD cell (or change the size of MD cell) and temperature. Fig. 1 presents simulated P–C isotherms for 10 nm, b.c.c. nanoparticles with potential parameters of $\varepsilon = 4$ and $\Delta r = -1 \text{ \AA}$. The isotherm slope is large at temperatures higher than 400 K, but it is fairly flat at temperatures lower than 200 K. Slant P–C isotherms were observed experimentally in Pd nanoparticles [8,9], which was considered to result from structural disorder at the particle surface. The plateau-like features at 100 K and 200 K in our result suggest that the disorder of the surface structure is less effective at lower temperatures in 10 nm particles.

Fig. 2 presents the potential parameter dependence of simulated P–C isotherm of 10 nm b.c.c. nanoparticles at 300 K. The energy parameter ε was changed to 1, 2, 4, 6, 8, and 10; the radius parameter Δr was kept to -1 \AA . The amount of absorbed hydrogen increases concomitantly with increasing ε until $\varepsilon = 8$, but decreases for $\varepsilon = 10$. The decrease of hydrogen absorption at high ε region results from blocking of the inward hydrogen diffusion by a hydrogen-rich surface layer as explained in the previous study [10]. The radius parameters smaller and larger than $\Delta r = -1 \text{ \AA}$ cause reduction of hydrogen absorption. Similar results to those shown in Figs. 1 and 2 were also observed in f.c.c. nanoparticle cases.

3.3. Particle size dependence

Yamauchi et al. [8,9] discussed the particle size dependence of hydrogen absorption in Pd nanoparticles. They showed that the slope of the P–C isotherm increases concomitantly with decreasing particle size. This result was explained by the structural disorder in surface region, which is larger in smaller particles of which the surface region is large compared to the bulk region. Fig. 3 presents modification of the metallic lattice attributable to hydrogenation in b.c.c. and f.c.c. nanoparticles of various sizes. It is known that the hydrogenated particles in some cases are strongly deformed from

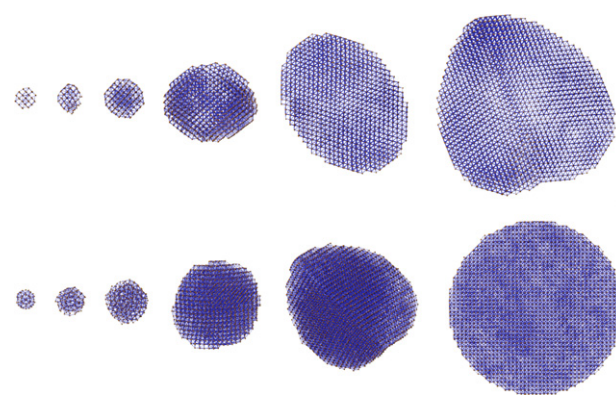


Fig. 3. Particle size dependencies of structural variation of b.c.c. (top) and f.c.c. (bottom) nanoparticles because of hydrogenation. Initial diameters of particles are 1, 1.4, 2, 4, 6, and 8 nm from left to right, and assumed conditions are $\varepsilon = 6$, $\Delta r = -1 \text{ \AA}$.

the original lattice and the particle shape (spheres or symmetric polyhedra). Uniaxial elongation and twin boundary generation in b.c.c. nanoparticles were observed. Those phenomena are considered to result from b.c.t. transformation. The smaller b.c.c. particles seem to maintain their b.c.c. lattices, although their surface structures are disordered.

Structural variation of f.c.c. nanoparticles by hydrogenation exhibits complex particle-size dependency: icosahedral lattice in smaller sizes than 1.4 nm, amorphous-like structures in 2 nm size, strongly deformed f.c.c. lattice in 4 nm size, f.c.c. lattices with a twin boundary in 6 nm size, and f.c.c. lattice in larger sizes. Such variation can be understood also by the surface effect and lattice transformation. Small f.c.c. clusters are known to have five-fold symmetries frequently. Pundt et al. [5,6] reported that hydrogenated nanoclusters smaller than 5 nm have five-fold structures. Generation of amorphous phase and lattice deformation in the middle size f.c.c. nanoparticles is created by the conflict between icosahedral and cubic symmetries, originally caused respectively by surface and bulk effects.

Fig. 4 presents simulated P–C isotherms of 4 nm b.c.c. nanoparticle in comparison with the 10 nm particle presented in Fig. 1. Curves of both sizes are almost identical at 600 K, but they are considerably different at lower temperatures. Hydrogen absorption at 400 K in 4 nm particles is less than that of 10 nm by about 0.1 in H/M at same hydrogen pressure. Similar size depen-

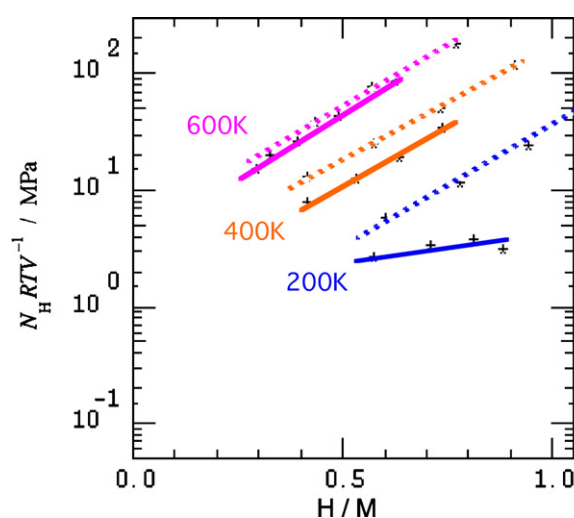


Fig. 4. Simulated P–C isotherms of 4 nm (dotted line) and 10 nm (solid line) b.c.c. nanoparticles at 200, 400 and 600 K. Assumed conditions are $\varepsilon = 4$, $\Delta r = -1 \text{ \AA}$.

dependency was observed for Pd nanoparticles by Yamauchi et al. [8,9]: hydrogen absorption decreases concomitantly with decreasing particle size. The difference between the simulated curves of two clusters becomes greater at 200 K. The curve slope at 200 K is almost flat for the 10 nm cluster. However, that of 4 nm maintains the same slope at higher temperatures. Similar results were obtained also in lower ε cases. These results suggest that the structural disorder by hydrogenation is more effective in smaller particles, especially at lower temperatures, than in larger ones.

4. Summary

Hydrogen absorption in metallic nanoparticles was investigated using classical MD simulation and parameter physics. Three patterns of hydrogen density profile in nanoparticles, non-absorbing, homogeneous absorbing, and that forming a hydrogen-rich surface layer appeared depending on the assumed potential parameter values. General features of P–C isotherms of nanoparticles including particle size dependency were reproduced by the simulation. Results show that strong M–H interaction leads to lattice deformation from b.c.c. to b.c.t., generation of grain boundary, and modification of the particle shape. Amorphization and grain boundary formation was observed in middle sized f.c.c. nanoparticles which might be related to the conflict between icosahedral and cubic symmetries.

Acknowledgment

This work has been supported by the New Energy and Industrial Technology Development Organization (NEDO) under “Advanced Fundamental Research Project on Hydrogen Storage Materials.”

References

- [1] T. Mutschele, R. Kirchheim, *Scr. Metall.* 21 (1987) 1101.
- [2] U. Stühr, H. Wipf, T.J. Udovic, J. Weissmüller, H. Gleiter, *J. Phys. Condens. Matter* 7 (1995) 219.
- [3] L. Zluski, A. Zaluska, J.O. Ström-Olsen, *J. Alloys Compd.* 253–4 (1997) 70.
- [4] H. Natter, B. Wetmann, B. Heisel, R. Hempelmann, *J. Alloys Compd.* 253–4 (1997) 84.
- [5] A. Pundt, C. Sachs, M. Winter, M.T. Reetz, D. Fritsch, R. Kirchheim, *J. Alloy Compd.* 293–5 (1999) 480.
- [6] M. Suleiman, N.M. Jisrawi, O. Dankert, M.T. Reetz, C. Bähz, R. Kirchheim, A. Pundt, *J. Alloy Compd.* 356–7 (2003) 644.
- [7] A. Pundt, R. Kirchheim, *Ann. Rev. Mater. Res.* 36 (2006) 555.
- [8] M. Yamauchi, R. Ikeda, H. Kitagawa, M. Tanaka, *J. Phys. Chem. C* 112 (2008) 3294.
- [9] M. Yamauchi, H. Kobayashi, H. Kitagawa, *Chem. Phys. Chem.* 10 (2009) 2566.
- [10] H. Ogawa, A. Tezuka, H. Wang, T. Ikeshoji, M. Katagiri, *Mater. Trans.* 49 (2008) 1983.
- [11] H. Ogawa, A. Tezuka, H. Wang, T. Ikeshoji, M. Katagiri, *Int. J. Nanosci.* 8 (2009) 39.
- [12] H. Ogawa, M. Kayanuma, M. Katagiri, *MRS Symp. Proc.* 1216E (2010), W03-02.
- [13] M.W. Finnis, J.E. Sinclair, *Phil. Mag. A* 50 (1984) 45.
- [14] G.J. Ackland, G. Tichy, V. Vitek, M.W. Finnis, *Phil. Mag. A* 56 (1987) 735.
- [15] M. Ruda, D. Farkas, J. Abriata, *Phys. Rev. B* 54 (1996) 9765.
- [16] R. Griessen, A. Driessen, *Phys. Rev. B* 30 (1984) 4372.